Proceedings of Ninth World Conference on Earthquake Engineering
August 2-9, 1988, Tokyo-Kyoto, JAPAN (Vol.III)

5-3-7

NONLINEAR PILE FOUNDATION MODEL FOR TIME-DOMAIN DYNAMIC RESPONSE ANALYSIS

Toyoaki NOGAMI[1], Kazuo KONAGAI[2] and Jun OTANI[3]

[1]Scripps Institution of Oceanography, Univ. of California, San Diego, La Jolla, California, USA
[2]Institution of Industrial Science, Univ. of Tokyo, Tokyo, Japan
[3]Department of Civil Engineering, Kyushu Univ., Fukuoka, Japan

SUMMARY

A time-domain Winkler soil-pile interaction model is developed from the dynamic response behavior of a cylindrical plane strain continuous medium. The model can rationally account for the slippage and gap at the soil-pile contact, inelastic soil behavior, dynamic condition and pile-soil-pile interaction. The model is verified by using a more rigorous analysis method and field pile load test results. Some numerical results are presented.

INTRODUCTION

Winkler soil model defined from the vibration behavior of a plane strain cylinder-medium system has been developed in the dynamic pile response analysis. This method is the most efficient in computation among various methods developed and yet can reproduce the dynamic pile behavior amazingly close to the one computed by using more rigorous methods (5). The time-domain model of this type has been developed recently by Nogami, et al. Such a time-domain model is essential for the analysis of nonlinear systems. The present paper describes the time-domain nonlinear soil-pile interaction models for both axial and flexural responses and presents some numerical results. Details and additional materials of the present paper can be found in Refs. 1 through 4.

SIMPLIFIED SOIL-PILE INTERACTION MODEL

Winkler model as shown in Fig. 1 is considered herein for reproducing the soil-pile interaction force in the dynamic response of pile foundations. At any given depth, this Winkler model consists of an interface element and a soil model. The interface element is the mechanism to produce the slippage and gap at the soil-pile contact. The pile-soil-pile interaction in a pile group is produced by the support motion at the fixed end of the Winkler model. In order to reproduce the nonlinear and dynamic conditions rationally, the soil model is formed by near-field and far-field elements connected in series as shown in Fig. 1. They reproduce respectively the nonlinear behavior and the behavior associated with the motions transmitted to the elastic region of the soil.

Near-Field Element The near-field element consists of one nonlinear spring, k_n, and consistent mass, $[m_n]$. The degradation effects are implemented in the nonlinear spring. The consistent mass matrix is defined assuming a linear variation of the near-field soil displacement with a radial distance from the center of the pile. The mass and stiffness matrices of this element are expressed as,

respectively

$$[m_n] = \frac{\pi r_0^2 \rho}{6}(r_1/r_0 - 1)\begin{bmatrix} r_1/r_0+3 & r_1/r_0+1 \\ r_1/r_0+1 & 3r_1/r_0+1 \end{bmatrix} \text{and } [k_n] = k_n \begin{bmatrix} 1 & -1 \\ -1 & 1 \end{bmatrix} \quad (1)$$

where r_0 and r_1 = radii of the pile and extent of the soil considered for the near-field, respectively; and ρ = mass of a unit volume of soil. The equation of motion of the near-field element is

$$(P_a(t),\ P_b(t))^T = [m_n](\ddot{u}_a(t),\ \ddot{u}_b(t))^T + [k_n](u_a(t),\ u_b(t))^T \quad (2)$$

where u_a and p_a = displacement and force at the end connected to the interface element; and u_b and p_b displacement and force at the outer end of the element.

Far-Field Element Reviewing the wave equation solutions obtained for a plane strain cylinder-medium system, simplified expressions are obtained in the frequency-domain for the force-displacement relationships of the far-field element. The plane strain cylinder-medium system above referred is a vertical massless rigid infinitely long cylinder in an infinite elastic medium. The radius of the cylinder corresponds to the radial extent of the near-field soil. The obtained expressions for vertical and horizontal motions are respectively

$$p(\omega) = \tilde{K}u(\omega) \quad \text{and} \quad p(\omega) = (\tilde{K} - m_f\omega^2)\ u(\omega) \quad (3)$$

where ω = circular frequency; $m_f = \xi_m(\nu_s)\ \rho\pi r_0^2$; $\xi_m(\nu_s)$ = factor given in Ref 4; and $1/\tilde{K} = \sum_{n=1}^{3} 1/(k_n + i\omega c_n)$

The values k_n and c_n are frequency independent parameters defined by k_1, k_2, $k_3) = G_s\ \xi_k(\nu_s)$ (3.518, 3.581, 5.529) and $(C_1, C_2, C_3) = G_s\xi_k\ (\nu_s)\ r_0/\beta$, (113.097, 25.133, 9.362), where $\xi_k(\nu_s)$= factor equal to 1 for vertical motion and factors given in Ref. 4 for horizontal motion. Eq. 3 indicates $\tilde{K}$ is the stiffness of the system consisting of three Voigt models connected in series. Thus, Eq. 3 implies the responses u are the responses of the systems shown in Fig. 2.

The response of the system considered for the vertical motion to the trapezoidal force, varying from p(0) to p(Δt) during the period from t=0 through t=Δt, can be expressed in an explicit form such that

$$u_n(t) = P(0)\ H_n(t) + P(\Delta t)\ I_n(t) \quad (4)$$

with $u(t) = \sum_{n=1}^{3} u_n(t)$, where being $\varepsilon_n = k_n/c_n$ and $\delta(t) = 1$ for $t>0$ and $= 0$ for $t<0$,

$$H_n(t) = \delta(t)\ \{\exp\ (\varepsilon_n\Delta t)/(\varepsilon_n\Delta t) - (1 + 1/(\varepsilon_n\Delta t))\}\ \exp\ (-\varepsilon_n t)/k_n$$

$$I_n(t) = \delta(t)\ \{(1-1/(\varepsilon_n\Delta t))\ \exp\ \{\varepsilon_n\Delta t) + 1/(\varepsilon_n\Delta t)\ \}\ \exp\ (-\varepsilon_n t)/k_n \quad (5)$$

A load time history is digitized at equal time interval Δt and linear variation with time is assumed. This load time history is considered to be a series of trapezoidal load time histories. Thus using Eq. 4 and manipulating, the response of the system considered for the vertical motion to this time history is obtained as

$$u_n(t_i) = u_n(t_{i-1})\ \exp\ (-\varepsilon_n\Delta t) + H_n(\Delta t)\ p(t_{i-1}) + I_n(\Delta t)p(t_i) \quad (6)$$

Rewriting Eq. 6, and using $u(t) = u_1(t) + u_2(t) + u_3(t)$, time-domain expressions for Eq. 3 are obtained respectively as

$$p(t_i) = k_f\ u(t_i) + d \quad \text{and} \quad p(t_i) = m_f\ddot{u}(t_i) + d \quad (7)$$

where $k_f = \sum_{n=1}^{3} 1/I_n(\Delta t)$; and $d = -k_f \sum_{n=1}^{3} \{u_n(t_{i-1}) \exp(-\varepsilon_n \Delta t) + H_n(\Delta t) p(t_{i-1})\}$

Support Motion The support motion is the motion transmitted from other piles. The time-domain expression of the support motion is developed from the frequency-domain analytical solutions obtained for the vibration of the plane strain cylinder-medium system considered in the development of the far-field element. Reviewing these analytical solutions, the following simplified expressions are developed in the frequency-domain:

$$u(\omega,r) = Q_1^{\beta}\,\phi_0^{\beta} \qquad \text{vertical motion}$$

$$\begin{cases} u(\omega,r) = Q_2^{\alpha}\,\phi_2^{\alpha}/\eta^2 - Q_2^{\beta}\,\phi_2^{\beta} + Q_1^{\alpha}\,\phi_1^{\alpha}/\eta^2 & \theta = 0^\circ \\ u(\omega,r) = -Q_2^{\alpha}\,\phi_2^{\alpha}/\eta^2 + Q_2^{\beta}\,\phi_2^{\beta} + Q_1^{\beta}\,\phi_1^{\beta} & \theta = 90^\circ \end{cases} \qquad \text{horizontal motion} \qquad (8)$$

where $\theta = 0^\circ$ and 90° correspond to the directions of the horizontal load and perpendicular to this direction, respectively; denoting $a_\beta = \omega r_0/\beta$ and $a_\alpha = \omega r_0/\alpha$ with α = P-wave velocity and β = S-wave velocity, $Q_1^{\alpha,\beta} = \sum_{n=1}^{3} 1/(k_n + i a_{\alpha,\beta} c_n)$ and $Q_2^{\alpha,\beta} = -(a_{\alpha,\beta}\,\bar{r})^{-2} + 1/(i a_{\alpha,\beta}\,\bar{r}) - \Sigma\, 1/(k_n' + i a_{\alpha,\beta} c_n')$; $\phi^{\alpha,\beta} = \exp\{-i a_{\alpha,\beta}(\bar{r}-1 - \psi_{\alpha,\beta})\}$ and $\phi_2^{\alpha,\beta} = \exp\{-i a_{\alpha,\beta}(\bar{r}-0.5 - \psi_{\alpha,\beta})\}$ with being $\psi_\alpha = -(\eta-1)/4, \psi_\beta = (\eta-1)/4\eta$ and $\eta = \sqrt{2(1-\nu_s)/(r-2\nu_s)}$. The values k_n, k_n', c_n and c_n' are given in Table 1.

An inverse Fournier transform of Eq. 8 leads to the response due to a unit impulse load. Integrating this expression with time, the response due to a trapezoidal load time history can be obtained. A piecewise linear time history is considered to be a series of trapezoidal time histories. Thus, superimposing the responses due to a series of trapezoidal load time histories and manipulating result in $u(t_i,r) = q_1^{\beta}(t_i,r)$ for vertical motion, and $u(t_i,r) = q_2^{\alpha}(t_i,r)/\eta^2 - q_2^{\beta}(t_i,r) + q_1^{\alpha}(t_i,r)/\eta^2$ and $u(t_i,r) = -q_2^{\alpha}(t_i,r)/\eta^2 + q_2^{\beta}(t_i,r) + q_1^{\beta}(t_i,r)$ for $\theta = 0^\circ$ and 90° horizontal motions, respectively, where $q_1^{\alpha,\beta} = \sum_{n=1}^{3} s_n^{\alpha,\beta}(t_i,r)$ and

$$q_2^{\alpha,\beta}(t_i,r) = \sum_{n=1}^{3} s_a^{\alpha,\beta}(t_i,r) + s_b^{\alpha,\beta}(t_i,r) - \sum_{n=1}^{3} s_n^{\alpha,\beta}(t_i,r) \qquad (9)$$

Each term at the right-hand side of Eq. 9 can be computed from the following expressions:

$$\begin{aligned} s_n^{\delta}(t_i,r) &= s_n^{\delta}(t_{i0-1},r)\exp(-\varepsilon_n\Delta t) + H_n(\Delta t,r)p(t_{i0-1}) + I_n(\Delta t,r)p(t_{i0}) \\ s_a^{\delta}(t_i,r) &= (1/2\pi)(\Delta t\delta/r)\sum_{j=1}^{i0-1} p(t_j) - (1/4\pi)(\Delta t\delta/r)\,p(t_{i0}) \\ s_b^{\delta}(t_i,r) &= s_b^{\delta}(t_{i0-1}) + (1/2\pi)(\Delta t\delta/r)\sum_{j=1}^{i0-1} p(t_j) - (1/2\pi)(\Delta t\delta/r)^2\,p(t_{i0-1}) \\ &\quad -(5/12\pi)(\Delta t\delta/r)^2\,p(t_{i0}) \qquad \delta = \alpha \text{ or } \beta \end{aligned} \qquad (10)$$

where $H_n(\Delta t,r)$ and $I_n(\Delta t,r)$ are identical to respectively $H_n(t)$ and $I_n(t)$ given in Eq. 5 but are dependent on r through k_n and c_n. In the above expression, the response due to the load applied at $t = t_{i0}$ arrives at r during the period between t_{i-1} and t_i. This requires $t_{i-1} < t_{i0} + \tau c \leq t_i$ in which $\tau c = r_0(\bar{r}-1)/\beta$ for vertical motion, $\tau_c = r_0(\bar{r}-1-\psi_{\alpha,\beta})$ for $q_1^{\alpha,\beta}$ and $\tau c = r_0(\bar{r}-0.5-\psi_{\alpha,\beta})$ for $q_2^{\alpha,\beta}$.

Interface element The mechanisms of the interface elements are shown in Fig. 3. In a vertical motion the slippage occurs at the soil-pile contact when maximum friction force reaches to the allowable force f_{max}. The interaction force is equal to f_{max} during the slippage. The contact condition resumes at any time during the slippage as soon as $\dot{U}-\dot{u}_a$ (where $\dot{U}$ = pile shaft velocity) becomes zero. The interface element for the horizontal motion consists of a rigid frame and

expansion joint. The expansion joint increases the opening of the frame by the plastic deformation of the soil. The amount of change in the opening is given by $\Delta\ddot{u}_{gap}(t_i) = \Delta u^p(t_i) \times (1-\beta)$, where Δu_{gap} = amount of change in opening, Δu^p = incremental plastic soil displacement and β = empirical factor.

EQUATION OF MOTION OF SOIL-PILE SYSTEM

The dynamic responses of a pile foundation are formulated by coupling the equation of motion of the pile shaft with that of the soil-pile interaction model. The solutions of the equations are given in Refs. 1 through 4.

ASSESSMENT OF APPROACH AND NUMERICAL RESULTS

The computed results by the proposed soil model are compared in Figs. 4 and 5 with those computed by the dynamic BEM-FEM analysis, in which the nonlinear finite element method is applied in the region within $6r_0$ and the boundary method is applied at the outer end of the finite element region. The nonlinear behavior of the near-field stiffness is defined from the static FEM analysis for a single cylinder. The proposed model can predict fairly well the responses of cylinders in both the elastic and inelastic continuous medium.

The statically applied cyclic load tests and vibration tests were conducted on an identical full-size pile at a common site. In order to assess the modeling concept proposed herein, the frequency-domain nonlinear soil-pile interaction model is also developed adopting the modeling concept proposed. The model parameters are determined from the static cyclic pile load test results. Then the pile responses in the vibration test are computed with this defined soil-pile interaction model. The computed results are compared with the field test results in Fig. 6. The soil-pile interaction model based on the proposed modeling concept can reasonably well predict the dynamic response of the pile in the field, once the model parameters are defined from the static conditions.

Fig. 7 shows the soil-pile interaction force for harmonic pile shaft displacement. The real and imaginary interaction forces are determined from those curves and are plotted in Fig. 8 for various harmonic displacement amplitudes. The imaginary part (damping) is reduced significantly at high frequencies when the nonlinearity develops.

Fig. 9 shows the complex stiffness of 2x2 pile computed for elastic and inelastic conditions. Under the inelastic condition, an elasto-plastic behavior is considered in the near-field element and the maximum force allowed in the near-field element spring (p^e) is assumed to increase linearly with depth. The nonlinearity induced in the soil reduces the pile-soil-pile interaction significantly.

CONCLUSIONS

The proposed soil-structure interaction model can rationally account for the gap and slippage at the soil-pile contact, the nonlinear soil behavior, the dynamic conditions, and the pile-soil-pile interaction. All of these are handled in the time-domain. The model is based on a Winkler's hypothesis and thus is very efficient in a computation.

REFERENCES

1. Nogami, T. and K. Konagai, "Time-Domain Axial Response of Dynamically Loaded Single Piles," Journal of Engineering Mechanics Division, ASCE, Vol. 113, No. GT2, 147-160, (1986).
2. Nogami, T. and K. Konagai, "Dynamic Axial Response of Nonlinear Pile Foundations," Journal of Geotechnical Engineering Division, ASCE, Vol. 113, No. GT2, 147-160, (1987).
3. Nogami, T., K. Konagai and J. Otani, "Time-Domain Dynamic Response of Nonlinear Pile Foundations," Report submitted to National Science Foundation, September, 1987, and also IMR Report No. 87-4, Institute of Marine Resources, University of California, (1987).
4. Nogami, T. and K. Konagai, "Time-Domain Flexural Response of Dynamically Loaded Single Piles," Journal of Engineering Mechanics Division, ASCE, Vol. 114, No. EM9, (1988).
5. Sanchez-Salinero, I., "Dynamic Stiffness of Pile Groups," Geotechnical Engineering Report GR83-5, Civil Engineering Dept., Univ. of Texas at Austin, July, 1983.

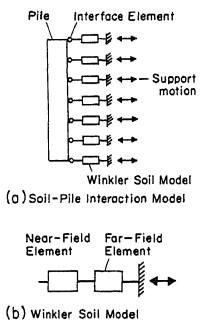

Fig. 1. Soil-pile interaction model and soil model

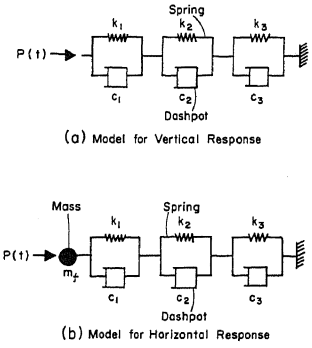

Fig. 2. Systems to produce far-field element behavior

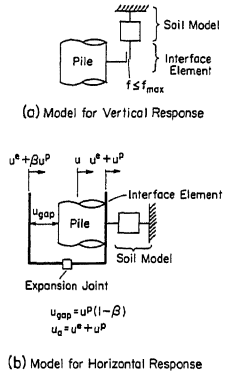

Fig. 3. Interface element model

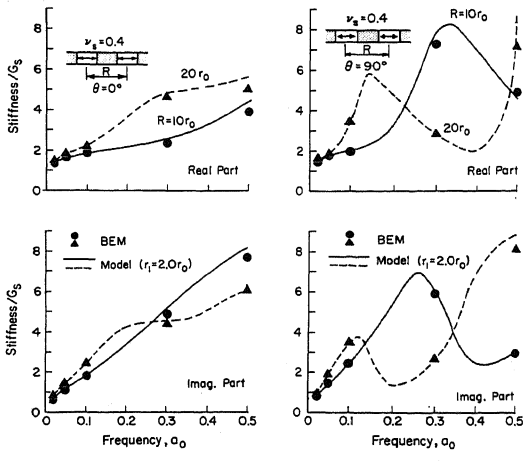

Fig. 4. Elastic stiffness of soil holding two piles

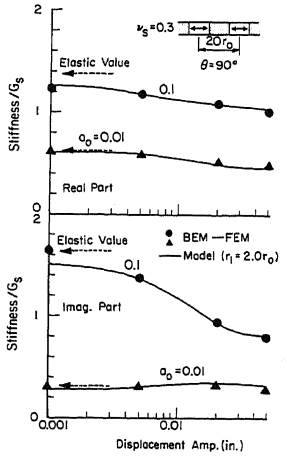

Fig. 5. Inelastic stiffness of soil holding two piles

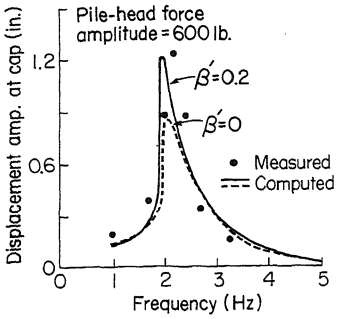

Fig. 6. Lateral pile cap displacement amplitudes computed and observed in vibration test

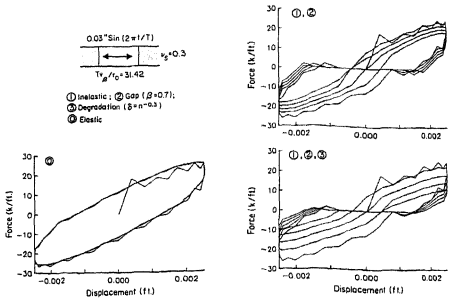

Fig. 7. Behavior of soil-pile interaction model for harmonic displacement excitation with constant amplitude

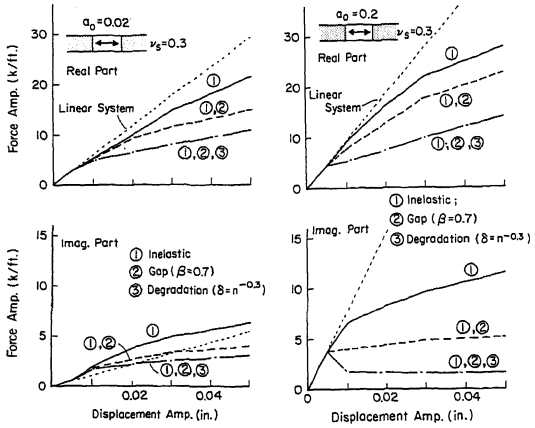

Fig. 8. Complex force amplitudes for harmonic displacement excitation with various amplitudes

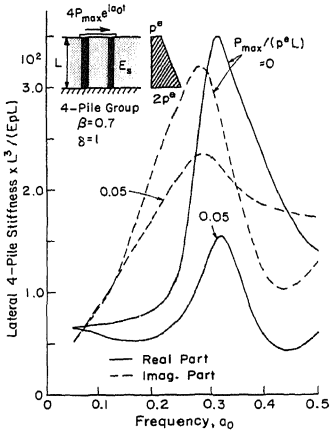

Fig. 9. Lateral stiffness of elastic and inelastic pile groups

Table 1

n	$(k_n/G_s)\cdot \bar{r}^{-0.5}$		$(c_n/G_s)\cdot \bar{r}^{-0.5}$	k_n'/G_s		c_n'/G_s	
1	$3.518\ \bar{r}^{-0.642}$	$\bar{r}<40$	113.097	$2.609 \log \bar{r} - 0.095$	$\bar{r}<40$	$-2.609 \log \bar{r} + 120.336$	$\bar{r}<40$
	0.3518	≥ 40		4.084	≥ 40	86.394	≥ 40
2	$3.581\ \bar{r}^{-0.359}$	$\bar{r}<28.6$	25.113	$9.400 \log \bar{r} - 3.110$	$\bar{r}<21.6$	$-6.262 \log \bar{r} + 31.395$	$\bar{r}<21.6$
	1.074	≥ 28.6		9.425	≥ 21.6	23.248	≥ 21.6
3	$5.529\ \bar{r}^{-0.162}$	$\bar{r}<5.44$	9.362	$29.223 \log \bar{r} + 2.205$	$\bar{r}<40$	$-4.175 \log \bar{r} + 17.370$	$\bar{r}<40$
	4.203	≥ 5.44		44.611	≥ 40	11.938	≥ 40